Visual Pattern Degradation based Image Quality Assessment

Jinjian Wu[a], Leida Li[b], Guangming Shi[a], Weisi Lin[c], and Wenfei Wan[a]

[a]School of Electronic Engineering, Xidian University, Xi'an, China;
[b]School of Information and Electrical Engineering,
China University of Mining and Technology, China;
[c]School of Computer Engineering, Nanyang Technological University, Singapore

ABSTRACT

In this paper, we introduce a visual pattern degradation based full-reference (FR) image quality assessment (IQA) method. Researches on visual recognition indicate that the human visual system (HVS) is highly adaptive to extract visual structures for scene understanding. Existing structure degradation based IQA methods mainly take local luminance contrast to represent structure, and measure quality as degradation on luminance contrast. In this paper, we suggest that structure includes not only luminance contrast but also orientation information. Therefore, we analyze the orientation characteristic for structure description. Inspired by the orientation selectivity mechanism in the primary visual cortex, we introduce a novel visual pattern to represent the structure of a local region. Then, the quality is measured as the degradations on both luminance contrast and visual pattern. Experimental results on Five benchmark databases demonstrate that the proposed visual pattern can effectively represent visual structure and the proposed IQA method performs better than the existing IQA metrics.

Keywords: Full-Reference, Image Quality Assessment, Visual Pattern, Orientation Selectivity

1. INTRODUCTION

In the multimedia era, objective image quality assessment (IQA) plays an important role in valid information selection from big data. During the past decade, a massive of IQA methods have been proposed for automatic quality measurement. As a simple metric with clear physical meaning, the peak signal-to-noise ratio (PSNR) is quite popular for quality measurement. However, it has been proved that this metric does not consistent well with the subjective perception.[1] Therefore, researchers tune to investigate the subjective perception of the human visual system (HVS), and try to mimic the subjective properties for quality assessment modeling.

Since the HVS is highly adaptive to extract structural information for image understanding, a structural similarity based quality assessment metric (SSIM)[2] is introduced, within which the degradation on structure (i.e., local luminance, variance, and covariance) is measured. Following this, a lot of structural similarity based IQA methods are proposed. Lin et al.[3] adopted the contrast and congruency for structure representation, and the quality is measured as the degradations on the two features. Liu et al.[4] and Zhu et al.[5] adopted the luminance change to represent the structure, and the degradation on the edge height or the gradient are computed to measure the quality, respectively. These structural degradation based IQA methods have greatly promote the accuracy of quality assessment. However, these methods measure the structure with only luminance contrast changes, they can be further improved by more information about images structures.

The interactions among pixels present the structure characteristic of images.[6,7] Moreover, visual cognition researches indicate that the HVS is sensitive to spatial luminance change and spatial orientation.[8,9] Thus, besides luminance contrast, distortions on spatial orientation will also degrade the structure of images, which result in quality degradation. Therefore, in this paper, we suggest to measure the structural degradations on both luminance contrast and spatial orientation for quality assessment.

The HVS presents obvious orientation selectivity mechanism for visual structure extraction.[10–12] Further studies on neuroscience indicates that orientation selectivity arises from the arrangement of excitatory and

E-mails: jinjian.wu@mail.xidian.edu.cn (J. Wu);lileida@cumt.edu.cn (L. Li); gmshi@xidian.edu.cn (G. Shi); wslin@ntu.edu.sg (W. Lin)

inhibitory interactions among neurons in a local receptive field of the primary visual cortex.[13,14] Moreover, neurons with similar preferred orientations present excitatory interaction, and neurons with dissimilar preferred orientations present inhibitory interaction.[15] Inspired by this, we calculate the preferred orientation of each pixel as its gradient direction. Then, we analyze the similarity of preferred orientations between a pixel and its circularly symmetric neighborhood to create an orientation selectivity based visual pattern (OSVP). With OSVP and luminance contrast, a novel structure descriptor is introduced.

With the novel structure descriptor, a new IQA method is proposed. Firstly, the structural degradation on luminance contrast is calculated. Next, the changes on OSVP types (shift from the original OSVP type to the distorted OSVP type) are measured. Then, the luminance contrast degradations on each pair of OSVP type shift are accumulated. Finally, the support vector regression (SVR) is employed for pooling the degradations on all pairs of OSVP shifts, and the quality of an image is returned.

2. QUALITY ASSESSMENT WITH STRUCTURE DEGRADATION

In this section, the structural degradations on luminance contrast and OSVP are separately measured. And then, by considering the degradations on the two features, the quality of an image is acquired.

2.1 Contrast Degradation

It is well known that the HVS is highly adapted to extract edge information for scene understanding, and is extremely sensitive to distortions on the edge. Thus, the distortion on edge is firstly calculated for structure degradation measurement. In this work, the edge magnitude is measured as luminance contrast ($\mathcal{L}_c$),

$$\mathcal{L}_c = \sqrt{\mathcal{L}_h^2 + \mathcal{L}_v^2}, \tag{1}$$

where $\mathcal{L}_h$ and $\mathcal{L}_v$ are the luminance contrast alone the horizontal and vertical directions, which can be computed as

$$\mathcal{L}_h = \mathcal{F} * f_h, \tag{2}$$
$$\mathcal{L}_v = \mathcal{F} * f_v, \tag{3}$$

where $\mathcal{F}$ is the input image, $*$ denotes the convolution operation, f_h and f_v are two filters alone horizontal and vertical orientations. Here, we adopt the Prewitt filters for luminance contrast computation,

$$f_h = \frac{1}{3}\begin{bmatrix} 1 & 1 & 1 \\ 0 & 0 & 0 \\ -1 & -1 & -1 \end{bmatrix}, \tag{4}$$
$$f_v = \frac{1}{3}\begin{bmatrix} 1 & 0 & -1 \\ 1 & 0 & -1 \\ 1 & 0 & -1 \end{bmatrix}. \tag{5}$$

Then, the structural degradation on luminance contrast is computed as the similarity between the reference and distorted images,

$$\mathcal{S}_l = \frac{2\mathcal{L}_c^r\mathcal{L}_c^d + c}{(\mathcal{L}_c^r)^2 + (\mathcal{L}_c^d)^2 + c} \tag{6}$$

where $\mathcal{S}_l$ is the contrast degradation, $\mathcal{L}_c^r$ is the luminance contrast of the reference image, $\mathcal{L}_c^d$ is the luminance contrast of the distorted image, and c is a small constant value to avoid the denominator being zero (we set c=0.1 in this work).

2.2 OSVP Degradation

The HVS presents obvious orientation selectivity for visual structure extraction, and is highly sensitive to degradations on orientation. Thus, the orientation selectivity mechanism is analyzed, and a novel OSVP is introduced for quality assessment.

The orientation selectivity mechanism arises from the arrangement of neuron interaction in the primary visual cortex. Moreover, the interaction type (excitatory and inhibitory interactions) decided by the similarity of the preferred orientation. By imitating this, we firstly compute the preferred orientation for each pixel,

$$\theta(x) = \arctan \frac{\mathcal{L}_v(x)}{\mathcal{L}_h(x)}, \tag{7}$$

where $\theta(x)$ is the preferred orientation of pixel x, $\mathcal{L}_h$ and $\mathcal{L}_v$ are the luminance contrast alone the horizontal and vertical directions, as computed in (2) and (5) respectively.

The interaction type $\mathcal{I}(x|x_i)$ is estimated as the similarity of the preferred orientations,

$$\mathcal{I}(x|x_i) = \begin{cases} 1 & \text{if } |\theta(x) - \theta(x_i)| < \mathcal{T} \\ 0 & \text{else} \end{cases}, \tag{8}$$

where '1' ('0') means excitatory (inhibitory) interaction, and $\mathcal{T}$ is the judging threshold and we set $\mathcal{T}$=6° here.

Finally, according to the arrangement of interactions between the central pixel and its symmetric neighbors (e.g., 8 symmetric neighbors), the OSVP of the pixel is acquired, OSVP=$\{\mathcal{I}(x|x_1), \mathcal{I}(x|x_2), \cdots, \mathcal{I}(x|x_N)\}$. In order to reduce the types of OSVP, we combine these patterns with the same number of excitatory interactions. As a result, for a N-neighbor OSVP, there are N+1 types of OSVP, whose excitatory interaction numbers are $0, 1, \cdots, N$. And in this paper,we name them as OSVP$_0$, OSVP$_1$, $\cdots$, OSVP$_N$.

With the degradation from distortion, the OSVP type for a pixel may shift from one type to another one. For example, the white noise may distort a plain region into a disorderly region, namely, shift from OSVP$_0$ into OSVP$_N$. Moreover, for M types of OSVP, there are M^2 pairs of OSVP shift, and each pair of OSVP shift represents different quality degradation.

2.3 Quality Assessment

Since different pair of OSVP shift results in different quality degradation, we accumulate the contrast degradations for each pair of OSVP shift,

$$\mathcal{D}(\mathrm{OSVP}^r_m, \mathrm{OSVP}^d_n) = \sum_{x=1}^{M} \mathcal{V}(x, m, n), \tag{9}$$

where $\mathcal{D}(\mathrm{OSVP}^r_m, \mathrm{OSVP}^d_n)$ is the accumulated contrast degradations from OSVP$_m$ to OSVP$_n$, M is the dimension of the image, $\mathcal{V}$ is the valid contrast degradations, which is calculated as

$$\mathcal{V}(x, m, n) = \begin{cases} \mathcal{S}_l(x) & \text{if } \mathrm{OSVP}^r(x){=}m, \mathrm{OSVP}^d(x){=}n \\ 0, & \text{else} \end{cases} \tag{10}$$

where $\mathcal{S}_l$ is the contrast degradation as computed in (6).

With (9) and (10), the contrast degradation on each pair of OSVP shift is computed. Then, we try to pool all pairs of OSVP shift to acquire the quality of an image. As an effective pooling procedure for high dimensional data, SVR is widely used in machine learning. Thus, the SVR is employed for feature pooling,

$$\mathcal{Q}(\mathcal{F}^r, \mathcal{F}^d) = \mathrm{SVR}\left(\mathcal{D}, \mathcal{MOD}\right), \tag{11}$$

where $\mathcal{Q}$ is the quality score, $\mathcal{D}$ is the structural degradation set defined as $\mathcal{D} = \{\mathrm{D}(\mathrm{OSVP}^r_m, \mathrm{OSVP}^d_n)|m = 0, \cdots N; n = 0, \cdots N\}$, and $\mathcal{MOD}$ is the model for regression.

3. EXPERIMENTAL RESULTS

In this section, the quality degradations caused by different types of distortion are firstly illustrated to demonstrate the proposed novel structure descriptor. Next, the performance of the proposed IQA method is verified by comparing with the state-of-the-art IQA metrics.

3.1 Effectiveness of The OSVP

The proposed descriptor presents the structure on both luminance contrast and orientation, which can effectively represent the degradation caused by different distortion types. As shown in Fig. 1, the *GIRL* image is distorted by three different types of distortion, namely, White noise (Fig. 1 (a) with MOS = 4.54), Gaussian blur (Fig. 1 (c) with MOS = 2.43), and JPEG noise (Fig. 1 (e) with MOS = 1.88). It is well known that different types of distortion generate different content degradations. As shown in Fig. 1 (a), the White noise adds disturbance into the image, which has limited effects on visual structure. The Gaussian blur smoothen these regions with luminance contrast, especially for the edge region, which mainly decrease the contrast value of visual structure. The JPEG noise not only removes some high frequency information but also generates artifacts; as a result, it decreases the contrast value of the edge region, and creates new edges in the smooth regions.

In order to illustrate the effects from different types of distortion, the degradations on luminance contrast is firstly analyzed. Here, the mean absolute different value of luminance contrast (we called LC) between the reference image and the distorted image is computed. For the three distorted images, Fig. 1 (a), (c), and (f), their corresponding LC values are 7.38, 6.78, and 8.16, respectively. According to the LC values, Fig. 1 (f) distorted by the JPEG noise has the largest degradation, and Fig. 1 (a) distorted by the White noise has larger degradation than that of Fig. 1 (c) distorted by the Gaussian blur. If we assess the quality with only the LC value, the result will conflict the ground truth (the MOS value, which shows that Fig. 1 (a) has the best quality, Fig. 1 (c) has better quality than Fig. 1 (e)). Therefore, the degradation on luminance contrast can not effectively represent the degradation on visual structure, and more other features should be considered for visual structure description.

In this work, we consider both luminance contrast and orientation for visual structure description. Different types of distortion will result in different degradation on each pair of OSVP shift. The structural degradation maps of these distorted images are shown in Fig. 1 (b), (d), and (f). As can be seen, the White noise obviously increases the luminance contrast value of the smooth region. As a result, the smooth region may be distorted into other types of regions, as shown in Fig. 1 (b), there are obvious changes on these bars corresponding to the 9th type of the reference OSVP (OSVP_8^r appears at the smooth region). On the contrary, the white noise mainly degrades the edge region. As a result, many regions may be degraded into smooth regions. As shown in Fig. 1 (d), there are obvious changes on these bars corresponding to the 9th type of the distorted OSVP (OSVP_8^d). Since the JPEG noise results in much complex distortion (degrades some edges and creates some new edge), the change on the structural degradation maps are much complex, which is quite different from that distorted by White noise and Gaussian blur, as shown in Fig. 1 (f). According to the above analysis, we can conclude that different types of distortion generate different degradations on luminance contrast and orientation; and therefore, the proposed structure descriptor can effectively represent visual degradation from different distortion types.

3.2 Performance Comparison on Databases

In this subsection, the proposed OSVP method are compared with 9 latest and state-of-the-art IQA methods, which are VSI,[16] GMSD,[17] IGM,[18] FSIM,[3] ADM,[19] GSIM,[4] MAD,[20] VIF,[21] and MSSIM.[2] In order to make a comprehensive comparison, 5 benchmark databases are adapted in this experiment: TID[22] database, which has 25 reference images and 1700 corresponding distorted images across 17 different types of distortion; CSIQ,[23] which has 30 reference images and 866 corresponding distorted images across 6 types of noise; LIVE,[24] which has 29 reference images and 799 corresponding distorted images across 5 types of noise; IVC,[25] which has 10 reference images and 185 corresponding distorted images across 4 types of noise; and TOY,[26] which has 28 reference images and 196 corresponding distorted images across 2 types of noise

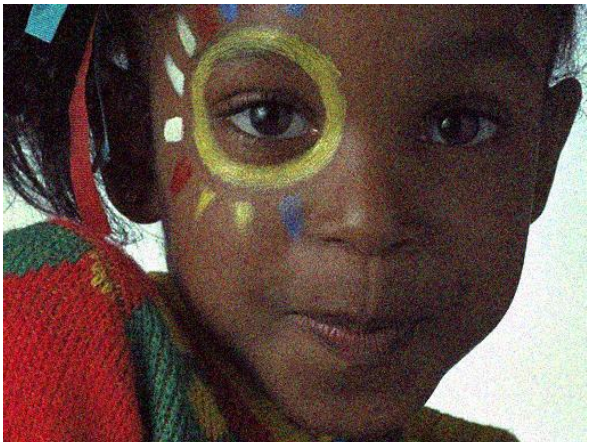

(a)

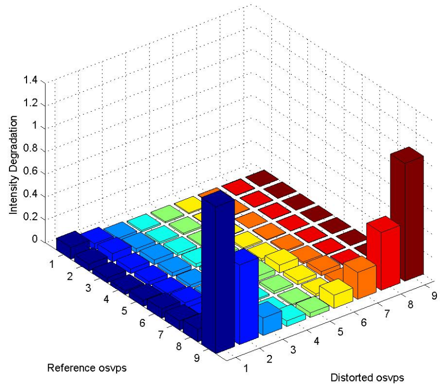

(b)

(c)

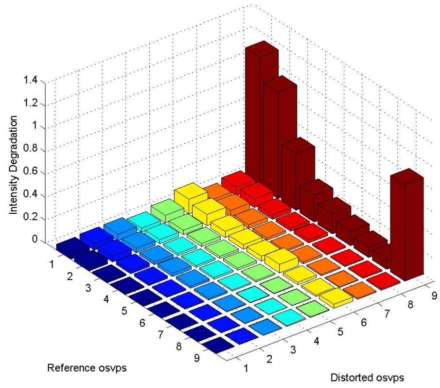

(d)

(e)

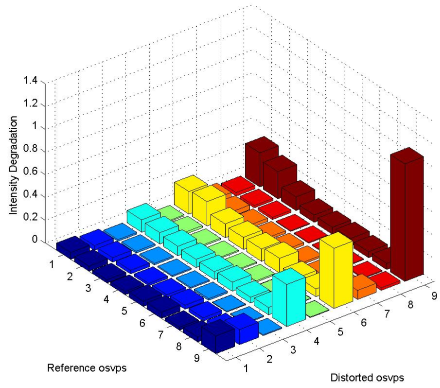

(f)

Figure 1: OSVP pair Shift under different types of distortion on *GIRL* image (with size 384×512). (a) White noise distorted image, MOS = 4.54. (c)Gaussian Blur distorted image, MOS = 2.43. (e) JPEG noise distorted image, MOS = 1.88. (b), (d), and (f) are their corresponding structure degradation maps.

Table 1: PERFORMANCE COMPARISON OF IQA METRICS ON 5 LARGE BENCHMARK DATABASES

DB	A. / C.	OSVP	VSI	GMSD	IGM	FSIM	ADM	GSIM	MAD	VIF	MSSIM
TID (1700)	PLCC	0.925	0.876	0.879	0.886	0.874	0.870	0.842	0.831	0.802	0.842
	SRCC	0.920	0.898	0.891	0.890	0.880	0.862	0.850	0.834	0.749	0.853
	RMSE	0.510	0.647	0.641	0.623	0.653	0.662	0.724	0.747	0.802	0.723
CSIQ (866)	PLCC	0.955	0.928	0.950	0.928	0.912	0.928	0.896	0.950	0.923	0.900
	SRCC	0.960	0.942	0.957	0.940	0.924	0.933	0.911	0.947	0.919	0.914
	RMSE	0.077	0.098	0.082	0.098	0.108	0.097	0.117	0.082	0.101	0.115
LIVE (799)	PLCC	0.965	0.938	0.957	0.957	0.960	0.936	0.944	0.967	0.960	0.941
	SRCC	0.965	0.952	0.960	0.958	0.963	0.946	0.956	0.967	0.963	0.945
	RMSE	7.174	9.457	7.965	7.925	7.677	9.619	9.012	6.923	7.669	9.266
IVC (185)	PLCC	0.934	0.912	0.923	0.913	0.938	0.913	0.939	0.921	0.903	0.893
	SRCC	0.913	0.899	0.914	0.903	0.926	0.903	0.929	0.915	0.896	0.884
	RMSE	0.416	0.500	0.467	0.497	0.423	0.496	0.419	0.475	0.524	0.548
TOY (168)	PLCC	0.921	0.898	0.890	0.899	0.925	0.953	0.943	0.952	0.932	0.916
	SRCC	0.908	0.893	0.883	0.891	0.918	0.940	0.930	0.938	0.918	0.905
	RMSE	0.502	0.580	0.601	0.578	0.501	0.401	0.440	0.402	0.478	0.531
Aver.	PLCC	0.941	0.910	0.920	0.917	0.922	0.920	0.913	0.924	0.904	0.898
	SRCC	0.938	0.917	0.921	0.916	0.922	0.917	0.915	0.920	0.889	0.900

In order to evaluate the performance of these IQA methods on a common space, a mapping function[18] is adopted to regress the computed quality score,

$$\mathcal{S}_r = \beta_1 \left(\frac{1}{2} - \frac{1}{1+\exp(\beta_2(\mathcal{S}_0 - \beta_3))} \right) + \beta_4\, \mathcal{S}_0 + \beta_5, \tag{12}$$

where $\{\beta_1, \beta_2, \beta_3, \beta_4, \beta_5\}$ are five parameters to be fitted.

To measure the conformity between the computed quality score and the ground truth (MOS), three classic performance criteria are adopted, namely, the Pearson linear correlation (PLCC), the Spearman rank-order correlation coefficient (SRCC), and the root mean squared error (RMSE).[18] A better IQA method will return larger PLCC and SRCC, and a smaller RMSE value. Since the proposed OSVP based IQA method employs the SVR procedure to measure image quality, 80% reference images and their corresponding distorted images are randomly selected to train the SVR model, and the rest images are chosen for test. Moreover, in order to eliminate the performance bias, the train-test procedure is repeated for 100 times, and the average performance is adopt for the final result.

The performance of there IQA methods are listed in Tab. 1. On TID database, the proposed method has much larger PLCC and SRCC values than all of the other methods, and has a much smaller RMSE value than the other one. According to the results on the three criteria, the proposed method performs obviously better than the other IQA methods on TID database. The performances on the CSIQ database are much similar with that on TID database, which shows that the proposed method performs the best on this database (has the largest PLCC and SRCC values, and smallest RMSE value). On LIVE and IVC databases, the proposed method has almost same PLCC, SRCC, and RMSE values with the best methods (i.e., on LIVE database, the PLCC, SRCC, and RMSE values of the best one (MAD) are 0.967, 0.967, and 6.923, respectively; and these values of the proposed method are 0.965, 0.965, and 7.174, respectively. On IVC database, these values of the best one (GSIM) are 0.939, 0.929, and 0.419, respectively; and these values of the proposed method are 0.934, 0.913, and 0.416, respectively). On TOY database, the proposed method performs slightly worse than the best one (ADM). Moreover, the average performance values on the five databases (we only list PLCC and SRCC values, while no RMSE, that is because the range of RMSE in these databases are quite different) are listed at the bottom of Tab. 1, which shows that the proposed method has much larger PLCC and SRCC values than any other IQA methods. Therefore, we can conclude that the proposed IQA method outperforms the latest and state-of-the-art IQA methods.

4. CONCLUSION

In this letter, we have proposed to represent the visual structure of an image with both luminance contrast and orientation, and introduced a novel OSVP based IQA method. It is well known that the HVS is highly adapt to extract structure from an image for scene perception, and the HVS is extremely sensitive to distortions on visual structure. However, how to effectively represent visual structure is still an open problem. Most existing IQA methods only calculate the degradation on luminance contrast for quality assessment. Inspired by the orientation selectivity mechanism in the primary visual cortex, we suggested to consider the orientation change caused by distortion. By imitating the excitatory and inhibitory interactions among nearby neurons, an OSVP is introduced to represent the orientation distribution of visual structure. Then, the degradations on both luminance contrast and orientation are measured. Finally, all features are pooled to return the quality. Experimental results on five databases have demonstrated that the proposed IQA method performs highly consistent with the subjective perception.

ACKNOWLEDGMENTS

This work was supported by the National Natural Science Foundation of China (Grant Nos. 61401325, 61472301, 61227004, 61301288),the Research Fund for the Doctoral Program of Higher Education (No. 20130203130001), the 111 Project (No. B07048), and the Fundamental Research Funds for The Central Universities (No. JB140227).

REFERENCES

1. Z. Wang and A. C. Bovik, "Mean squared error: Love it or leave it?," *IEEE Signal Processing Magazine* **26**, pp. 98–117, Jan. 2009.
2. Z. Wang, A. Bovik, H. Sheikh, and E. Simoncelli, "Image quality assessment: from error visibility to structural similarity," *Image Processing, IEEE Transactions on* **13**(4), pp. 600–612, 2004.
3. L. Zhang, L. Zhang, X. Mou, and D. Zhang, "FSIM: a feature similarity index for image quality assessment," *Image Processing, IEEE Transactions on* **20**, pp. 2378–2386, Aug. 2011.
4. A. Liu, W. Lin, and M. Narwaria, "Image quality assessment based on gradient similarity," *Image Processing, IEEE Transactions on* **21**, pp. 1500–1512, Apr. 2012.
5. J. Zhu and N. Wang, "Image quality assessment by visual gradient similarity," *Image Processing, IEEE Transactions on* **21**, pp. 919 –933, Mar. 2012.
6. J. Wu, F. Qi, and G. Shi, "Self-similarity based structural regularity for just noticeable difference estimation," *Journal of Visual Communication and Image Representation* **23**(6), pp. 845–852, 2012.
7. J. Wu, W. Lin, G. Shi, X. Wang, and F. Li, "Pattern masking estimation in image with structural uncertainty," *IEEE Transactions on Image Processing* **22**(12), pp. 4892–4904, 2013.
8. J. G. Daugman, "Uncertainty relation for resolution in space, spatial frequency, and orientation optimized by two-dimensional visual cortical filters," *Journal of the Optical Society of America. A, Optics and Image Science* **2**, pp. 1160–1169, July 1985.
9. R. L. Buckner and F. M. Krienen, "The evolution of distributed association networks in the human brain," *Trends in Cognitive Sciences* **17**, pp. 648–665, Dec. 2013.

10. D. H. Hubel and T. N. Wiesel, “Receptive fields, binocular interaction and functional architecture in the cat’s visual cortex,” *The Journal of Physiology* **160**(1), pp. 106–154, 1962.
11. D. H. Hubel and T. N. Wiesel, “Receptive fields and functional architecture in two nonstriate visual areas (18 and 19) of the cat,” *Journal of neurophysiology* **28**, pp. 229–289, 1965.
12. T. D. Albright, “Direction and orientation selectivity of neurons in visual area MT of the macaque,” *Journal of neurophysiology* **52**(6), pp. 1106–1130, 1984.
13. T. W. Troyer, A. E. Krukowski, N. J. Priebe, and K. D. Miller, “Contrast-invariant orientation tuning in cat visual cortex: Thalamocortical input tuning and correlation-based intracortical connectivity,” *The Journal of Neuroscience* **18**(15), pp. 5908–5927, 1998.
14. B. Chapman, K. R. Zahs, and M. P. Stryker, “Relation of cortical cell orientation selectivity to alignment of receptive fields of the geniculocortical afferents that arborize within a single orientation column in ferret visual cortex,” *The Journal of neuroscience: the official journal of the Society for Neuroscience* **11**(5), pp. 1347–1358, 1991.
15. D. Ferster and K. D. Miller, “Neural mechanisms of orientation selectivity in the visual cortex,” *Annual review of neuroscience* **23**, pp. 441–471, 2000.
16. L. Zhang, Y. Shen, and H. Li, “VSI: A visual saliency-induced index for perceptual image quality assessment,” *IEEE Transactions on Image Processing* **23**, pp. 4270–4281, Oct. 2014.
17. W. Xue, L. Zhang, X. Mou, and A. Bovik, “Gradient magnitude similarity deviation: A highly efficient perceptual image quality index,” *IEEE Transactions on Image Processing* **23**, pp. 684–695, Feb. 2014.
18. J. Wu, W. Lin, G. Shi, and A. Liu, “Perceptual quality metric with internal generative mechanism,” *IEEE Transactions on Image Processing* **22**, pp. 43 –54, Jan. 2013.
19. S. Li, F. Zhang, L. Ma, and K. N. Ngan, “Image quality assessment by separately evaluating detail losses and additive impairments,” *Multimedia, IEEE Transactions on* **13**, pp. 935–949, Oct. 2011.
20. E. C. Larson and D. M. Chandler, “Most apparent distortion: full-reference image quality assessment and the role of strategy,” *Journal of Electronic Imaging* **19**, p. 011006, 2010.
21. H. R. Sheikh and A. C. Bovik, “Image information and visual quality,” *Image Processing, IEEE Transactions on* **15**, pp. 430–444, Feb. 2006.
22. N. Ponomarenko and K. Egiazarian, “Tampere image database 2008 tid2008.”
23. E. C. Larson and D. M. Chandler, “Categorical image quality (csiq) database.”
24. H. R. Sheikh, K. Seshadrinathan, A. K. Moorthy, Z. Wang, A. C. Bovik, and L. K. Cormack, “Image and video quality assessment research at live.”
25. A. Ninassi, P. L. Callet, and F. Autrusseau, “Subjective quality assessment-ivc database.”
26. Y. Horita, K. Shibata, Y. Kawayoke, and Z. M. P. Sazzad, “Mict image quality evaluation database.”